Article

Not peer-reviewed version

Role of Vaccination on the Co-Infection Model with COVID-19 Associated with Diabetes

Md. Abdul Hye * , Md. Haider Ali Biswas , Mohammed Forhad Uddin

Posted Date: 19 June 2024

doi: 10.20944/preprints202406.1320.v1

Keywords: COVID-19; Diabetes; Comorbidity; Co-infection; Vaccination; Numerical Simulation.

 doi:10.20944/preprints202406.1320.v1

Article

Role of Vaccination on the Co-Infection Model with COVID-19 Associated with Diabetes

Md. Abdul Hye [1,2,*], Md. Haider Ali Biswas [3] and Mohammed Forhad Uddin [2]

[1] Department of Mathematics and Statistics, Bangladesh University of Business and Technology (BUBT), Dhaka-1216, Bangladesh. Email: abdul@bubt.edu.bd
[2] Department of Mathematics, Bangladesh University of Engineering and Technology (BUET), Dhaka-1000, Bangladesh. Email: farhad@math.buet.ac.bd
[3] Mathematics Discipline, Khulna University, Khulna-9208, Bangladesh. Email: mhabiswas@yahoo.com
* Correspondence: abdul@bubt.edu.bd

Abstract: COVID-19 infection is extremely dangerous for persons with comorbidities such as kidney disease and diabetes. Although many people of all ages and socioeconomic backgrounds have suffered due to this pandemic, those with underlying medical conditions like kidney disease and diabetes are more vulnerable to becoming infected with COVID-19 related to weak immunity. However, the role of vaccination in the co-infection of COVID-19 with diabetics is not available in the literature. Therefore, we examine the unique challenges presented by the co-infection of COVID-19 in individuals with diabetes, focusing on its disease transmission dynamics. A mathematical modelling technique is to be employed in this work to analyse the dynamics of COVID-19 outbreaks with seven compartments, including vaccination with comorbidities such as diabetes. We also investigated analytically by displaying the solutions' existence, boundedness, positivity and sensitivity. After calculating the basic reproduction numbers, the stability analysis of model equilibrium points is also covered. If the reproduction numbers are less than unity, the disease-free equilibrium points of the model appear to be both locally and globally stable. The findings of this study are that as the vaccination rate rises, the incidence of COVID-19 and its co-infections with diabetes decreases. Effective disease treatment strategies may be based partly on the possible impact of vaccination on the co-infection of COVID-19 related to diabetic disease insights.

Keywords: COVID-19; Diabetes; Comorbidity; Co-infection; Vaccination; Numerical Simulation

1. Introduction

COVID-19, caused by the SARS-CoV-2 virus, emerged as a significant global health threat in late 2019 [1]. Identified initially in Wuhan, Hubei province of China, the disease quickly spread globally, leading the World Health Organization (WHO) to declare it a pandemic in March 2020. The virus's origins have been the subject of extensive research, with studies suggesting that it likely jumped from an animal host, potentially bats, to humans, possibly with an intermediate host involved [2]. The primary transmission mode is through respiratory droplets, although contact with contaminated surfaces can also result in infection [3]. The disease manifests symptoms from mild cough and fever to severe respiratory distress, with older adults and those with underlying health conditions particularly vulnerable [4]. COVID-19 has had profound global implications, affecting public health systems, economies, and daily lives. Efforts to combat its spread have included worldwide vaccination campaigns, the efficacy of which has been a primary focus of scientific research and public health initiatives [5]. While there hasn't been an approved vaccine or antiviral treatment for COVID-19, many countries and people have adopted non-pharmaceutical measures like wearing face masks in public, practising social distancing, and enforcing lockdowns to help curb the spread of the virus. [6,7]. Recent epidemiological research suggests that it's important to consider the co-existence of COVID-19 and comorbidities like diabetes, lung disease, and heart disease. Individuals with these

 doi:10.20944/preprints202406.1320.v1

underlying conditions appear to have a heightened risk of contracting the virus [8,9]. Bjorgul, Novicoff and Saleh [10] characterise comorbidities as diseases or medical conditions that coexist with the primary diagnosis under consideration while not sharing an origin or causal relationship. A mathematical model assessing the impact of comorbidity on COVID-19 dynamics, revealing that strategies preventing infection in individuals with comorbidities, particularly diabetes, are the most cost-effective as presented in [32]. In line with the Centers for Disease Control and Prevention (CDC), individuals of any age with conditions such as chronic kidney disease, COPD (chronic obstructive pulmonary disease), a weakened immune state from a solid organ transplant, obesity (defined by a body mass index [BMI] of 30 or above), serious heart conditions like heart failure and coronary artery disease, Type 2 diabetes mellitus, hypertension or high blood pressure, and neurological conditions like dementia are at a heightened risk of experiencing severe complications from COVID-19 [11]. A clinical study reported as [12] further reinforces this understanding. In an examination of 41 confirmed COVID-19 patients, it was found that thirteen of them had pre-existing conditions such as hypertension, chronic obstructive pulmonary disease, cardiovascular disease, and diabetes. The transmission methods for infectious diseases have also been outlined in various studies, as indicated in [13,14].

In Nigeria, it has been observed that individuals with diabetes mellitus are more susceptible to contracting COVID-19. Studies suggest that those with severe COVID-19 symptoms have a higher incidence of diabetes mellitus than those with milder symptoms [4]. The WHO recently cautioned that no conclusive evidence suggests that individuals who have recovered from COVID-19 are immune to a second infection [15].

Models play a pivotal role in understanding the transmission dynamics of infectious diseases. The utilization of mathematical models for examining infectious diseases has seen a marked rise in recent periods, as indicated by studies [16,17]. Hence, the emergence of a branch has been done, which is called mathematical epidemiology. Frequent diagnostic tests, the availability of clinical data, and electronic surveillance have facilitated mathematical models' applications to critically examine scientific hypotheses and design real-life strategies for controlling diseases [18].

According to WHO, the COVID-19 vaccine is highly effective, but a small percentage of people will still get ill from COVID-19 after vaccination [19–21]. Everybody could also pass the virus on to others who are not vaccinated. Mathematical models provided invaluable insights into potential transmission dynamics, peak infection times, and the potential impact of interventions [22]. These models also identified key parameters like the basic reproduction number (R_0) and offered scenarios based on various containment strategies. The complexities surrounding COVID-19 transmission dynamics, co-infections, and their impact on global health have necessitated mathematical modelling as an essential tool in understanding and predicting disease trends [23–25]. Recently, researchers have significantly contributed to the mathematical modelling of COVID-19 co-infections with other diseases. Askari et al.[26] , reported a groundbreaking understanding of the co-infections between COVID-19 and kidney disorders. It was observed that kidney disorders may exacerbate the progression of the COVID-19 disease. Dadashi et al. [27] explored the co-infection rates of COVID-19 and influenza during the flu season. Mousquer et al. [28] investigated the implications of co-infection of COVID-19 and tuberculosis in patients with compromised lung function. Omame et al. [16] conducted a study on co-infection transmission involving COVID-19 and diabetes in unvaccinated individuals. Hence, current research needs to address more comprehensively the intricacies of COVID-19 co-infections with diseases like diabetes. When juxtaposed with a contagious disease like COVID-19, many of these chronic and acute conditions offer a complex picture of public health. These interrelations, explored through mathematical models, have proved invaluable in shaping the global response and will continue to play a pivotal role in future public health crises.

This study investigates into the intricacies of these co-infections and will explore vaccination aimed at mitigating the severity and spread of the diseases. Therefore, conducting focused, comprehensive studies on these co-infections remains a crucial objective in our continued fight against the COVID-19 pandemic. A compartmental epidemic model with vaccination that cannot produce 100% immunity, analytical analysis of the model, numerical simulation, and discussions.

 doi:10.20944/preprints202406.1320.v1

This study explores the comparative dynamics of coronavirus disease with vaccination among individuals with or without comorbidity (diabetes mellitus).

2. Model Formulation

We delved into a seven-compartment model for a randomised human population. The entire group is split into seven distinct categories, namely susceptible population (S), COVID-19 infected (I_C), covid-19 vaccinated susceptible (V) diabetic sensitive individuals (S_d), Co infected Covid-19 and diabetics(I_{cd}), Recover from Covid-19 (R_c), Recover from Covid-19 but with people with diabetes (R_{cd}).

We assumed that the recruitment increases the susceptible population at a rate Δ. All populations in each compartment suffer from a natural death rate μ. The susceptible population (S) acquires COVID-19 at the rate $f = \frac{\alpha(I_c+\gamma I_{cd})}{N}$, where α indicates the COVID-19 contact rate, γ Parameter alteration for higher infectiousness of co-infected persons due to comorbidity. Diabetes is becoming more common among people at this epidemiological rate at ϕ . Diabetes development rate θ in vaccinated susceptible persons. Vaccinated susceptible (V) acquire COVID-19 at a decreased rate$(1-\sigma)f$, where σ is the COVID-19 vaccine efficacy. COVID-19 vaccination rate τ_v from the susceptible populations. Diabetic susceptible (S_d) acquire COVID-19 at the rate ωf , where ω accounts for diabetics' greater susceptibility rate. χ_1, χ_2 indicate recovery metrics for COVID-19 based on individual groupings (I_C) and Covid-19 co-infected (I_{cd}) respectively. Reinfection rates η_1, η_2 for Individuals recovered from COVID-19 are in compartments R_c and R_{cd} respectively.

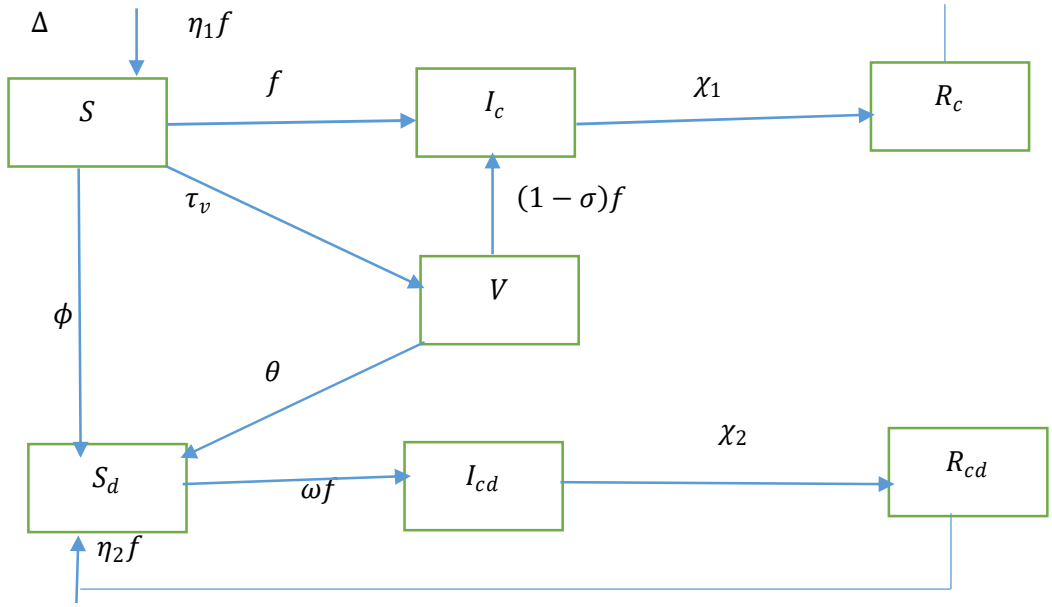

Figure 1. The transmission dynamics of diabetes and COVID-19 co-infection are shown in a flow chart.

$$\frac{ds}{dt} = \Delta - fS - \tau_v S - \phi S - \mu S + +\eta_1 f R_c \quad (1)$$
$$\frac{ds_d}{dt} = \phi S + \theta V - \omega f S_d + +\eta_2 f R_{cd} - \mu S_d \quad (2)$$
$$\frac{dI_c}{dt} = fS + (1-\sigma)fV - \chi_1 I_c - \mu I_c \quad (3)$$
$$\frac{dI_{cd}}{dt} = \omega f S_d - \chi_2 I_{cd} - \mu I_{cd} \quad (4)$$
$$\frac{dV}{dt} = \tau_v S - \theta V - (1-\sigma)fV - \mu V \quad (5)$$
$$\frac{dR_c}{dt} = \chi_1 I_c - \eta_1 f R_c - \mu R_c \quad (6)$$
$$\frac{dR_{cd}}{dt} = \chi_2 I_{cd} - \eta_2 f R_{cd} - \mu R_{cd} \quad (7)$$

 doi:10.20944/preprints202406.1320.v1

Table 1. Parameter description with values.

Parameter	Biological Interpretation	Value	References
Δ	Recruitment rate to susceptible populations	630	calculated
τ_v	Vaccination rate COVID-19 (rate of people who are vaccinated)	0.25	[4]
α	COVID-19 contact rate	1.2	Fitted
γ	Parameter alteration for higher infectiousness of co-infected persons due to comorbidity	0.5776	Fitted
σ	COVID-19 vaccine efficacy	0.70	[3]
η_1	The compartment R_C indicates the reinfection rates η_1 for individuals recovered from COVID-19.	0.0013	Estimated
η_2	The compartment R_{Cd} indicates the reinfection rates η_2 for individuals recovered from COVID-19.	0.0013	Estimated
ω	Accounts for diabetics' greater susceptibility rate.	0.60	[1]
ϕ	Rate of Diabetes development for susceptible humans	0.0028	Estimated
θ	Diabetes increased rate θ in vaccinated susceptible persons	0.018	Fitted
χ_1	Recovery rates for COVID-19 within the I_C compartment.	0.00014	Fitted
χ_2	Recovery rates for COVID-19 within the I_{Cd} compartment.	0.0124	Fitted
μ	Natural death rate	*0.000038*	calculated

 doi:10.20944/preprints202406.1320.v1

Theorem 1. All the populations of the system with positive initial conditions are nonnegative let $S > 0, S_d > 0, V \geq 0, I_c \geq 0, I_{cd} \geq 0, R_c \geq 0, R_{cd} \geq 0$, then $(S, S_d, V, I_c, I_{cd}, R_c, R_{cd})$ of the system are positive for all time $t > \mathbf{0}$.

$$\frac{ds}{dt} = \Delta - fS - \tau_v S - \phi S - \mu S + \eta_1 f R_c$$

By using the technique of variable separation $\frac{dS}{dt}$ can be reduced to

$$\frac{dS}{dt} > -(f + \tau_v + \phi + \mu)S$$

$$\frac{dS}{S} > -(f + \tau_v + \phi + \mu)dt$$

Then, the above equation is integrated to yield the solution below

$S(t) > S_0 e^{-\int_0^t (f+\tau_v+\phi+\mu)dt} > 0$ (8)

Since the initial value, $S(0)$ and the exponential functions in equation (8) are always positive

Hence, $S(t)$is positive. Using a similar technique to verify other equations of equations (1) to (7), this shows that

$$S > 0, S_d > 0, V \geq 0, I_c \geq 0, I_{cd} \geq 0, R_c \geq 0, R_{cd} \geq 0$$

Theorem 2. The dynamical system (1) to (7) is positively invariant in the closed invariant set $Z_1 = \{(S, S_d, V, I_c, I_{cd}, R_c, R_{cd}) \in \mathbb{R}_+^7 : N \leq \frac{\Delta}{\mu}\}$

To obtain an invariant region that shows that the solution is bounded, we have

$$N = S + S_d + V + I_c + I_{cd} + R_c + R_{cd}$$

$$\frac{dN}{dt} = \frac{dS}{dt} + \frac{dS_d}{dt} + \frac{dV}{dt} + \frac{dI_c}{dt} + \frac{dI_{cd}}{dt} + \frac{dR_c}{dt} + \frac{dR_{cd}}{dt}$$

$$\begin{aligned}\frac{dN}{dt} = {} & \Delta - fS - \tau_v S - \phi S - \mu S + \phi S + \theta V - \omega f S_d - \mu S_d + fS + (1-\sigma)fV - \chi_1 I_c + \eta_1 f R_c - \mu I_c \\ & + \omega f S_d + \eta_2 f R_{cd} - \chi_2 I_{cd} - \mu I_{cd} + \tau_v S - \theta V - (1-\sigma)fV - \mu V + \chi_1 I_c - \eta_1 f R_c - \mu R_c \\ & + \chi_2 I_{cd} - \eta_2 f R_{cd} - \mu R_{cd}\end{aligned}$$

$\frac{dN}{dt} = \Delta - N\mu$

The general solution of the equation

$N(t) = \frac{\Delta}{\mu} + \left(N(0) - \frac{\Delta}{\mu}\right) e^{-\mu t}$, where $N(t) = N(0)$ at $t = 0$

We can follow that $N(t) \to \frac{\Delta}{\mu}$ as $t \to \infty$. Thus, it can be concluded that $N(t)$ is bounded as $0 \leq N(t) \leq \frac{\Delta}{\mu}$.

Hence, the feasible region of the model in the nonnegative region is defined as

$Z = \{(S, S_d, V, I_c, I_{cd}, R_c, R_{cd}) \in \mathbb{R}_+^7 + : N \leq \frac{\Delta}{\mu}\}$ (9)

3. Analytical Analysis of Co-Infection Model

We compute the equilibrium and provide conditions for their existence. We also determine the reproduction number of the model and use it to study the stability of the computed equilibria and the sensitivity of the model.

3.1. The Disease-Free Steady-State Equilibrium Points of the Model

The disease-free equilibrium of equations (1) to (7) are given by

$$I_c = 0, I_{cd} = 0, R_c = 0, R_{cd} = 0$$

$$\frac{dS}{dt} = \frac{dS_d}{dt} = \frac{dV}{dt} = \frac{dI_c}{dt} = \frac{dI_{cd}}{dt} = \frac{dR_c}{dt} = \frac{dR_{cd}}{dt} = 0$$

$$S = \frac{\Delta}{(\tau_v + \phi + \mu)}$$

$$S_d = \frac{\Delta\phi(\theta+\mu)(\tau_v+\phi+\mu) + \theta\tau_v\Delta}{\mu(\tau_v+\phi+\mu)^2(\theta+\mu)}$$

$$V = \frac{\tau_v \Delta}{(\theta+\mu)(\tau_v+\phi+\mu)}$$

Hence, the disease-free equilibrium point (DFEP) of the COVID-19 co-infection model is

$\left(\frac{\Delta}{(\tau_v+\phi+\mu)}, \frac{\Delta\phi(\theta+\mu)(\tau_v+\phi+\mu)+\theta\tau_v\Delta}{\mu(\tau_v+\phi+\mu)^2(\theta+\mu)}, \frac{\tau_v\Delta}{(\theta+\mu)(\tau_v+\phi+\mu)}, 0, 0, 0, 0\right)$ (10)

 doi:10.20944/preprints202406.1320.v1

3.2. The Basic Reproduction Number R_0

$$\frac{dI_c}{dt} = fS + (1-\sigma)fV - \chi_1 I_c + \eta_1 f R_c - \mu I_c$$

$$\frac{dI_{cd}}{dt} = \omega f S_d + \eta_2 f R_{cd} - \chi_2 I_{cd} - \mu I_{cd}$$

$$F_1 = \frac{\alpha(I_c + \gamma I_{cd})}{N} S + (1-\sigma)\frac{\alpha(I_c + \gamma I_{cd})}{N} V$$

$$F_2 = \omega \frac{\alpha(I_c+\gamma I_{cd})}{N} S_d$$

$$V_1 = (\chi_1 + \mu) I_c \ , \ V_2 = (\chi_2 + \mu) I_{cd}$$

$$F = \begin{pmatrix} \frac{\partial F_1}{\partial I_c} & \frac{\partial F_1}{\partial I_{cd}} \\ \frac{\partial F_2}{\partial I_c} & \frac{\partial F_2}{\partial I_{cd}} \end{pmatrix}$$

$$F = \begin{pmatrix} \frac{\alpha S + (1-\sigma)\alpha V}{N} & \frac{\alpha\gamma S + (1-\sigma)\gamma\alpha V}{N} \\ \frac{\omega\alpha S_d}{N} & \frac{\omega\alpha\gamma S_d}{N} \end{pmatrix}$$

$$V = \begin{pmatrix} (\chi_1 + \mu) & 0 \\ 0 & (\chi_2 + \mu) \end{pmatrix}$$

$$V^{-1} = \begin{pmatrix} \frac{1}{(\chi_1 + \mu)} & 0 \\ 0 & \frac{1}{(\chi_2 + \mu)} \end{pmatrix}$$

$$FV^{-1} = \begin{pmatrix} \frac{\alpha S + (1-\sigma)\alpha V}{N} & \frac{\alpha\gamma S + (1-\sigma)\gamma\alpha V}{N} \\ \frac{\omega\alpha S_d}{N} & \frac{\omega\alpha\gamma S_d}{N} \end{pmatrix} \begin{pmatrix} \frac{1}{(\chi_1 + \mu)} & 0 \\ 0 & \frac{1}{(\chi_2 + \mu)} \end{pmatrix}$$

$$= \begin{pmatrix} \frac{\alpha S + (1-\sigma)\alpha V}{N(\chi_1 + \mu)} & \frac{\alpha\gamma S + (1-\sigma)\gamma\alpha V}{N(\chi_2 + \mu)} \\ \frac{\omega\alpha S_d}{N(\chi_1 + \mu)} & \frac{\omega\alpha\gamma S_d}{N(\chi_2 + \mu)} \end{pmatrix}$$

$$FV^{-1} - \lambda I = \begin{pmatrix} \frac{\alpha S + (1-\sigma)\alpha V}{N(\chi_1 + \mu)} - \lambda & \frac{\alpha\gamma S + (1-\sigma)\gamma\alpha V}{N(\chi_2 + \mu)} \\ \frac{\omega\alpha S_d}{N(\chi_1 + \mu)} & \frac{\omega\alpha\gamma S_d}{N(\chi_2 + \mu)} - \lambda \end{pmatrix}$$

The largest eigenvalue is the basic reproduction number.

$$R_0 = max\left(\frac{\alpha S + (1-\sigma)\alpha V}{N(\chi_1 + \mu)}, \frac{\omega\alpha\gamma S_d}{N(\chi_2 + \mu)}\right) \quad (11)$$

3.3. Stability Analysis at Disease-Free Equilibrium Point

The disease-free equilibrium is locally asymptotically stable if $R_0 < 1$, and unstable if $R_0 > 1$.

Jacobian matrix of the system (1) to (7)

$$J = \begin{pmatrix} -(f+\tau+\mu+\phi) & 0 & -\frac{\alpha S}{N} & -\frac{\alpha\gamma S}{N} & 0 & 0 & 0 \\ \phi & -(\omega f + \mu) & -\frac{\omega S_d}{N} & -\frac{\omega\gamma S_d}{N} & \theta & 0 & 0 \\ f & 0 & \frac{(1-\sigma)V + \eta_1 R_c}{N} - (\chi_1 + \mu) & \frac{(1-\sigma)\gamma V + \eta_1\gamma R_c}{N} & (1-\sigma)f & \eta_1 f & 0 \\ 0 & \omega f & \frac{\omega S_d + \eta_2 R_{cd}}{N} & \frac{\omega\gamma S_d + \eta_2\gamma R_{cd}}{N} - (\chi_2 + \mu) & 0 & 0 & \eta_2 f \\ \tau_v & 0 & -\frac{(1-\sigma)V}{N} & -\frac{(1-\sigma)\gamma V}{N} & -(\theta + \mu + (1-\sigma)f) & 0 & 0 \\ 0 & 0 & \chi_1 - \frac{\eta_1 R_c}{N} & -\frac{\eta_1\gamma R_c}{N} & 0 & -(\eta_1 f + \mu) & 0 \\ 0 & 0 & -\frac{\eta_2 R_{cd}}{N} & \chi_2 - \frac{\eta_2\gamma R_{cd}}{N} & 0 & 0 & -(\eta_1 f + \mu) \end{pmatrix}$$

At the disease-free equilibrium point

 doi:10.20944/preprints202406.1320.v1

$$\left(\frac{\Delta}{(\tau_v+\phi+\mu)}, \frac{\Delta\phi(\theta+\mu)(\tau_v+\phi+\mu)+\theta\tau_v\Delta}{\mu(\tau_v+\phi+\mu)^2(\theta+\mu)}, \frac{\tau_v\Delta}{(\theta+\mu)(\tau_v+\phi+\mu)}, 0,0,0,0\right)$$

$$J = \begin{pmatrix} -\Pi_1 & 0 & -\frac{\alpha S}{N} & -\frac{\alpha\gamma S}{N} & 0 & 0 & 0 \\ \phi & -\mu & -\frac{\omega S_d}{N} & -\frac{\omega\gamma S_d}{N} & \theta & 0 & 0 \\ f & 0 & \frac{(1-\sigma)V}{N} - \Pi_2 & \frac{(1-\sigma)\gamma V}{N} & 0 & 0 & 0 \\ 0 & \omega f & \frac{\omega S_d}{N} & \frac{\omega\gamma S_d}{N} - \Pi_3 & 0 & 0 & 0 \\ \tau_v & 0 & -\frac{(1-\sigma)V}{N} & -\frac{(1-\sigma)\gamma V}{N} & -\Pi_4 & 0 & 0 \\ 0 & 0 & \chi_1 & 0 & 0 & -\mu & 0 \\ 0 & 0 & 0 & \chi_2 & 0 & 0 & -\mu \end{pmatrix}$$

where,

$\Pi_1 = (\tau + \mu + \phi), \Pi_2 = (\chi_1 + \mu), \Pi_3 = (\chi_2 + \mu), \Pi_4 = (\theta + \mu)$ and the solution of Polynomial characteristic

$$A^2 + \left(\Pi_1 + \Pi_3 - \frac{\alpha(1-\sigma)V+\alpha S_d+\alpha S}{N}\right)A + \Pi_1\Pi_3(1-R_0) = 0 \quad (12)$$

Utilising the Routh-Hurwitz criterion, if $R_0 < 1$, equation (12) will only have roots with negative real parts. Consequently, the disease-free equilibrium J is locally stable when $R_0 < 1$.

3.4. Endemic Equilibrium Analysis

For the equilibrium points of the equations (1) to (7),

$$\frac{dS}{dt} = \frac{dS_d}{dt} = \frac{dV}{dt} = \frac{dI_c}{dt} = \frac{dI_{cd}}{dt} = \frac{dR_c}{dt} = \frac{dR_{cd}}{dt} = 0$$

Let $E^* = (S^*, S_d^*, V^*, I_c^*, I_{cd}^*, R_c^*, R_{cd}^*)$ represents the disease equilibrium point. The components of E^* are the positive solutions of the nonlinear system of equations

$$\Delta - fS - \tau S - \phi S - \mu S = 0$$
$$\phi S + \theta V - \omega f S_d - \mu S_d = 0$$
$$fS + (1-\sigma)fV - \chi_1 I_c + \eta_1 f R_c - \mu I_c = 0$$
$$\omega f S_d + \eta_2 f R_{cd} - \chi_2 I_{cd} - \mu I_{cd} = 0$$
$$\tau_v S - \theta V - (1-\sigma)fV - \mu V = 0$$
$$\chi_1 I_c - \eta_1 f R_c - \mu R_c = 0$$
$$\chi_2 I_{cd} - \eta_2 f R_{cd} - \mu R_{cd} = 0$$

$$S^* = \frac{\Delta}{\left(\frac{\alpha(I_c^* + \gamma I_{cd}^*)}{N} + \tau + \phi + \mu\right)}$$

$$S_d^* = \frac{\phi S^* + \theta V^*}{\left(\omega\frac{\alpha(I_c^* + \gamma I_{cd}^*)}{N} + \mu\right)}$$

$$I_c^* = \frac{\frac{\alpha(I_c^* + \gamma I_{cd}^*)}{N} S^* + (1-\sigma)\frac{\alpha(I_c^* + \gamma I_{cd}^*)}{N} V^* + \eta_1 \frac{\alpha(I_c^* + \gamma I_{cd}^*)}{N} R_c^*}{(\chi_1 + \mu)}$$

$$I_{cd}^* = \frac{\omega\frac{\alpha(I_c^* + \gamma I_{cd}^*)}{N} S_d^* + \eta_2 \frac{\alpha(I_c^* + \gamma I_{cd}^*)}{N} R_{cd}^*}{(\chi_2 + \mu)}$$

$$V^* = \frac{\tau_v S^*}{\left(\theta + (1-\sigma)\frac{\alpha(I_c^* + \gamma I_{cd}^*)}{N} + \mu\right)}$$

$$R_c^* = \frac{\chi_1 I_c^*}{\left(\mu + \eta_1 \frac{\alpha(I_c^* + \gamma I_{cd}^*)}{N}\right)}$$

$$R_{cd}^* = \frac{\chi_2 I_{cd}^*}{\left(\eta_2 \frac{\alpha(I_c^* + \gamma I_{cd}^*)}{N} + \mu\right)}$$

Theorem 3. The endemic equilibrium point $E^* = (S^*, S_d^*, V^*, I_c^*, I_{cd}^*, R_c^*, R_{cd}^*)$ is locally stable when the basic reproduction number $R_0 > 1$.

 doi:10.20944/preprints202406.1320.v1

3.5. Global Stability of DFE and the EE Point

$$T = S - S^* - S^* \ln\left(\frac{S}{S^*}\right) + \frac{1}{2} I_c^2$$

$$\frac{dT}{dt} = \left(1 - \frac{S^*}{S}\right)\frac{dS}{dt} + I_c \frac{dI_c}{dt}$$

$$= \left(1 - \tfrac{S^*}{S}\right)[\Delta - (f + \theta + \mu)S] + I_c[fS - P_1 I_c]$$

$$= \left(1 - \frac{S^*}{S}\right)[\Delta - (f + \theta + \mu)S] + I_c^2[\frac{\alpha S}{N} - P_1]$$

At the COVID-19 free equilibrium point (CFE) we have the following form

$$\frac{dT}{dt} = -\frac{(f + \theta + \mu)(S - S^*)^2}{S} + I_c^2(\frac{\alpha S}{N} - P_1)$$

$$\leq -\frac{(f + \theta + \mu)(S - S^*)^2}{S} + \frac{I_c^2}{P_1}(R_{0c} - 1)$$

Hence, $T < 0$ if and only if $R_{0c} \leq 1$. Therefore, L is a Lyapunov function for the system (1) to (7). It follows by the La Salle's Invariance Principle [24], that the CFE of the model (1) to (7) are globally

The lyapunov function is defined as

$$L = \frac{1}{2}[(S - S^*) + (S_d - S_d^*) + (V - V^*) + (I_c - I_c^*) + (I_{cd} - I_{cd}^*) + (R_c - R_c^*) + (R_{cd} - R_{cd}^*)]^2$$

The function L needs to be proven to determine whether the Lyapunov function is valid or invalid for Ψ^*

$$L(\Psi^*) = L(S^*, S_d^*, V^*, I_c^*, I_{cd}^*, R_c^*, R_{cd}^*)$$

$$L(\Psi^*) = \frac{1}{2}[(S - S^*) + (S_d - S_d^*) + (V - V^*) + (I_c - I_c^*) + (I_{cd} - I_{cd}^*) + (R_c - R_c^*) + (R_{cd} - R_{cd}^*)]^2$$

It is proven that $L(\Psi^*) = 0$

$$L(\Psi) = \frac{1}{2}[(S - S^*) + (S_d - S_d^*) + (V - V^*) + (I_c - I_c^*) + (I_{cd} - I_{cd}^*) + (R_c - R_c^*) + (R_{cd} - R_{cd}^*)]^2$$

Because $\forall\ (S, S_d, V, I_c, I_{cd}, R_c, R_{cd}) \neq (, S_d^0, V^0, I_c^0, I_{cd}^0, R_c^0, R_{cd}^0)$, so that it is showed that $L(\Psi) > 0$.

$$\frac{dL}{dt} = [(S - S^*) + (S_d - S_d^*) + (V - V^*) + (I_c - I_c^*) + (I_{cd} - I_{cd}^*) + (R_c - R_c^*) + (R_{cd} - R_{cd}^*)] + \frac{d}{dt}[S + S_d + V + I_c + I_{cd} + R_c + R_{cd}]$$

$$= [(S - S^*) + (S_d - S_d^*) + (V - V^*) + (I_c - I_c^*) + (I_{cd} - I_{cd}^*) + (R_c - R_c^*) + (R_{cd} - R_{cd}^*)][\Delta - \mu(S + S_d + V + I_c + I_{cd} + R_c + R_{cd})]$$

Let

$$\Delta = \mu(S^* + S_d^* + V^* + I_c^* + I_{cd}^* + R_c^* + R_{cd}^*)]$$

Now, $= [(S - S^*) + (S_d - S_d^*) + (V - V^*) + (I_c - I_c^*) + (I_{cd} - I_{cd}^*) + (R_c - R_c^*) + (R_{cd} - R_{cd}^*)] \times [-\mu((S - S^*) + (S_d - S_d^*) + (V - V^*) + (I_c - I_c^*) + (I_{cd} - I_{cd}^*) + (R_c - R_c^*) + (R_{cd} - R_{cd}^*)]$

$$= -[(S - S^*) + (S_d - S_d^*) + (V - V^*) + (I_c - I_c^*) + (I_{cd} - I_{cd}^*) + (R_c - R_c^*) + (R_{cd} - R_{cd}^*)] \times [\mu((S - S^*) + (S_d - S_d^*) + (V - V^*) + (I_c - I_c^*) + (I_{cd} - I_{cd}^*) + (R_c - R_c^*) + (R_{cd} - R_{cd}^*)]$$

Based on the description above, it can be concluded that $\frac{dL}{dt} < 0$ if $R_0 > 1$ and $\frac{dL}{dt} = 0$ if $S = S^*, S_d = S_d^*, V = V^*, I_c = I_c^*, I_{cd} = I_{cd}^*, R_c = R_c^*, R_{cd} = R_{cd}^*$. Hence, by LaSalle's invariance principle, it means that the endemic equilibrium point in the spread o fCOVID-19 is globally asymptotically stable if R0>1.

3.6. Sensitivity Analysis

The sensitivity index quantifies the relative variation in a state variable in response to a parameter modification and is determined using sensitivity analysis. Using the method developed by Chitnis et al. [28], we calculate the sensitivity indices of R_0 to the model parameters. These indices highlight the significance of each aspect in the dynamics and prevalence of disease transmission. Sensitivity analysis is used to identify the most relevant elements that impact the community's ability to contain and spread infection. We apply the technique offered to do sensitivity analysis.

$$R_0 = \frac{\alpha\Delta(\theta + \mu + \tau_v - \sigma\tau_v)}{N(\chi_1 + \mu)(\theta + \mu)(\tau_v - \sigma\tau_v)}$$

$$\beta_l^{R_0} = \frac{\partial R_0}{\partial l} \times \frac{l}{R_0}$$

Preprints.org (www.preprints.org) | NOT PEER-REVIEWED | Posted: 19 June 2024 doi:10.20944/preprints202406.1320.v1

$$\beta_{\alpha}^{R_0} = \frac{\partial R_0}{\partial \alpha} \times \frac{\alpha}{R_0}$$

$$\beta_{\alpha}^{R_0} = \frac{S + (1-\sigma)V}{N(\chi_1 + \mu)} * \frac{1}{\frac{S + (1-\sigma)V}{N(\chi_1 + \mu)}} = +1 > 0$$

$$\beta_{\sigma}^{R_0} = -\frac{V}{1} * \frac{\sigma}{S+(1-\sigma)V} = -\frac{\sigma\tau_v}{\theta+\mu+\tau_v-\sigma\tau_v}$$

$$\beta_{\tau_v}^{R_0} = \frac{-\frac{\alpha\Delta}{(\tau_v+\phi+\mu)^2} + \frac{\alpha\Delta(1-\sigma)(\theta+\mu)}{(\theta+\mu)(\tau_v+\phi+\mu)^2}}{N(\chi_1+\mu)} * \frac{\tau_v}{\alpha\frac{\Delta}{(\tau_v+\phi+\mu)} + (1-\sigma)\alpha\frac{\tau_v\Delta}{(\theta+\mu)(\tau_v+\phi+\mu)}}{N(\chi_1+\mu)}$$

$$\beta_{\tau_v}^{R_0} = \frac{-\tau_v\sigma(\theta+\mu)}{(\tau_v+\phi+\mu)(\theta+\mu-\tau_v-\sigma\tau_v)}$$

$$\beta_{\theta}^{R_0} = \frac{-\alpha\Delta}{(\theta+\mu)^2 N(\chi_1+\mu)} * \frac{\theta}{\frac{\alpha\Delta(\theta+\mu+\tau_v-\sigma\tau_v)}{N(\chi_1+\mu)(\theta+\mu)(\tau_v-\sigma\tau_v)}} = \frac{-\theta(\tau_v-\sigma\tau_v)}{(\theta+\mu)(\theta+\mu+\tau_v-\sigma\tau_v)}$$

$$\beta_{\chi_1}^{R_0} = -\frac{\alpha\Delta(\theta+\mu+\tau_v-\sigma\tau_v)}{N(\chi_1+\mu)^2(\theta+\mu)(\tau_v-\sigma\tau_v)} * \frac{\chi_1}{\frac{\alpha\Delta(\theta+\mu+\tau_v-\sigma\tau_v)}{N(\chi_1+\mu)(\theta+\mu)(\tau_v-\sigma\tau_v)}} = -\frac{\chi_1}{(\chi_1+\mu)}$$

The sensitivity indices in Table 2 are described as follows: for parameters with positive indices, the corresponding basic reproduction number increases (decreases) as those parameters increase (decreases). On the other hand, negative indices suggest that as those parameters increase, the associated basic reproduction number decreases, and vice versa. According to Table 2, 10% increase or reduction of α causes 10% increase or reduction in the value of R_0, 10% increase or reduction of ω causes 10 % increase or decrease in the value of R_0, 10% increase or reduction of θ causes 1.1% increase or decrease in the value of R_0, 10% increase or reduction of σ causes 1.6% reduction or increase in the value of R_0, 10% increase or reduction of γ causes 10% reduction or increase in the value of R_0, 10% increase or reduction of χ_1 causes 9.4 % reduction or increase in the value of R_0, and 10% increase or reduction of τ_v causes 4.2 % reduction or increase in the value of R_0.

Table 2. Sensitivity indices of R_0 on parameters for co-infection model.

Parameter	Sensitivity index
α	*+1.0000*
σ	*−0.1605*
τ_v	*−0.4240*
θ	*−0.1068*
χ_1	−0.9482
ω	*+1.0000*
γ	*+1.0000*

Sensitivity analysis was conducted using the partial rank correlation coefficients (PRCCs) combined with the Latin hypercube sampling to assess the influence of each model parameter on the initial spread of the disease, represented by R_0 . Figure 2 illustrates the PRCCs, highlighting the ramifications of altering input parameters on the basic reproduction number, R_0. Parameters that have positive PRCCs enhance the initial transmission rates, whereas those with negative PRCCs curtail R_0. A closer look at Figure 2 helps pinpoint the most impactful parameters. Table 2's sensitivity indices reveal that when the values of α, ω, and γ surge, and other parameters remain constant, there's an uptick in R_0, suggesting increased disease endemicity due to the positive indices. Conversely, when the parameters σ, τ_v, θ, and χ_1 drop and other values remain unchanged, R_0 diminishes, indicating a decline in disease endemicity given the negative indices. The contact rate α and the higher infectiousness of the co-infected person's rate γ are the most sensitive parameters.

Preprints.org (www.preprints.org) | NOT PEER-REVIEWED | Posted: 19 June 2024 doi:10.20944/preprints202406.1320.v1

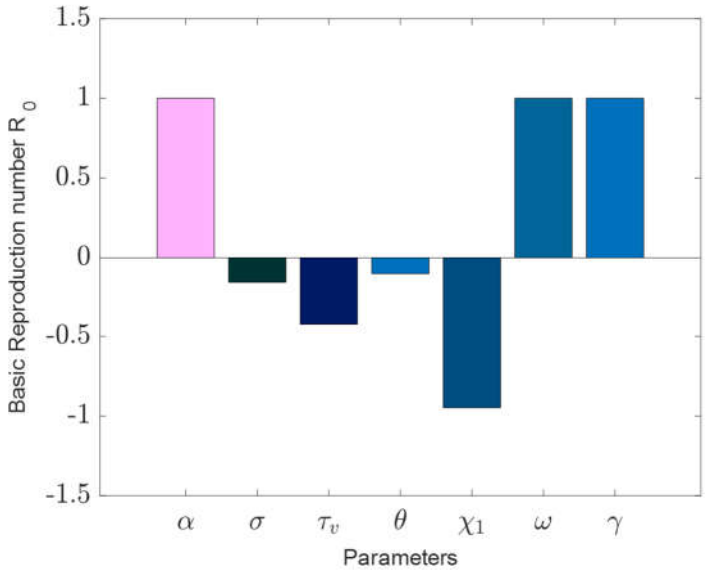

Figure 2. Effects of parameters variation on R_0.

3.7. Data Fitting and Parameters

The population of Bangladesh, as cited in source [26], is approximately 170000000. Additionally, referencing a study by Dahiru et al. [29], which investigated the prevalence of diabetes mellitus in Bangladesh, we set specific initial conditions in our analysis of COVID-19 in the region. Considering the first infected in Bangladesh, we try to explore the dynamics of worldwide daily and cumulative cases from April 2020. The data is retrieved from the World Health Organization (WHO) 's website [26]: $S(0)$ = 0.93 * 170000000: This represents the initial number of susceptible individuals without comorbidities, calculated as 93% of the total population.$S_d(0)$ = 0.07 * 1700000: This denotes the initial number of susceptible individuals with comorbidities at 7% of the total population.$I_c(0)$ = 412320: This indicates the initial number of COVID-19 cases without comorbidities. $I_{cd}(0)$ = 0: This is the initial number of recovered individuals from COVID-19 without comorbidities. $R_c = 0$: This signifies the initial number of COVID-19 cases with comorbidities. $R_{cd}(0)$ = 0: This represents the initial number of recovered individuals from COVID-19 with comorbidities. In our analysis, two optimisation algorithms were utilised for data fitting purposes. The objective function is root mean error square $= \sqrt{\sum_{data\ i}^{n}(\boldsymbol{I_{C\ actual}(t_i) - I_{C\ model}(t_i)})^2}$ .The first was the genetic algorithm (GA), and the second was the fmincon algorithm, as documented in references [30,31].

This led to the calculation of the natural mortality rate per month as the inverse of life expectancy, resulting in a value of $\mu = \frac{1}{72.72\times365} = 0.000038$. Furthermore, the recruitment rate was approximated by manipulating the ratio of $\frac{\nabla}{\mu}$ to yield the initial population, resulting in $\nabla = 630$ individuals per day. Due to limited data on co-infections, we estimated certain co-infection-related parameters, while others were deduced from actual data. During the estimation process, the initial conditions of the state variables were set as delineated in Table 1.

The Figure 4(a) represents the cumulative COVID-19 infected population from April 2020 to October 2020 [26]. This period captures data before the implementation of COVID-19 vaccinations. The green dots indicate the real data collected during this time frame, while the brown line represents the fitted model without vaccination. The graph shows a clear increase in the number of COVID-19 cases, reflecting the natural progression of the pandemic before any vaccination measures were in place. The close fit between the model and the real data demonstrates the model's accuracy in predicting the spread of COVID-19 in the absence of vaccinations.

 doi:10.20944/preprints202406.1320.v1

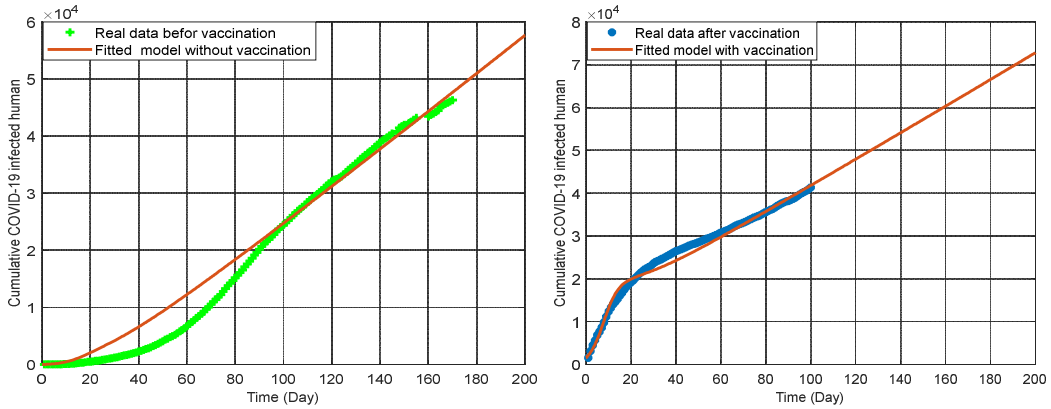

Figure 4. (a) Fitting the cumulative number of confirmed cases of COVID-19 before vaccination with the model vaccination rate $\tau_v = 0$. (b) Fitting the cumulative number of confirmed cases of COVID-19 after vaccination with the model vaccination rate $\tau_v \neq 0$.

The graph 4(b) represents the cumulative COVID-19 infected population from September 2021 to April 2022 [26], which covers the period after the implementation of COVID-19 vaccinations. The blue dots indicate the real data collected during this period, and the brown line represents the fitted model with vaccination. This graph shows a significant change in the infection trend compared to the pre-vaccination period. The data indicates that vaccination has played a crucial role in reducing the number of new infections and controlling the spread of the virus. The fitted model closely aligns with the real data, highlighting the model's effectiveness in capturing the impact of vaccination on the COVID-19 pandemic.

These graphs collectively illustrate the dramatic difference in COVID-19 infection trends before and after vaccination. The pre-vaccination period saw a steady rise in infections, accurately captured by the model. In contrast, the post-vaccination period shows a controlled infection rate, demonstrating the critical role of vaccination in managing and reducing the spread of COVID-19. These findings underscore the importance of vaccination campaigns in mitigating the impact of the pandemic and provide valuable insights for public health strategies in regions like Bangladesh. Additionally, the data shows that increasing vaccination rates not only decrease the number of COVID-19 cases but also reduce the incidence of co-infections with comorbidities, thereby improving overall public health outcomes. This highlights the dual benefit of vaccinations in controlling the pandemic and managing chronic health conditions.

4. Numerical Result and Discussions

The model's analytical outcomes can be visualized through numerical simulations using parameter values sourced from existing literature. For system analysis, the ODE113 solver from MATLAB is utilized. A simulation of the Co-infection Model is carried out in vaccination treatments to examine how the key determinants may affect the transmission of COVID-19 in diabetics and non-diabetics. The Co-infection Model following vaccine interventions has a disease-free equilibrium that is locally asymptotically stable when the related effective reproduction number, R_0 is available. COVID-19 would be removed from the population if the initial conditions shifted toward the disease-free equilibrium point. Based on the findings, it can be believed that only the COVID-19 recovery rate will improve with immunization.

From Figure 5(a) and 5(b), we see that the susceptible people are monotonically declining. At the same time, the number of comorbid susceptible people initially keeps rising, but after a few days, it gradually falls. In Figure 5(d) and 5(e), since the start of this pandemic, the COVID-19 infected curve and the co-infected curve have progressively climbed, but after a few days, both curves have unexpectedly increased as well. On the other hand, the COVID-19 vaccination rate presented in 5(c) is also higher than the recovery rate for people mentioned in 5(f) and 5(g). According to the graph's

 doi:10.20944/preprints202406.1320.v1

dynamic nature, it is predicted that until a vaccination or appropriate treatment is introduced, the sick people will continue to develop. Even yet, it can be managed by preserving physical distances, raising the vaccination rate, and creating a self-immunity system, as revealed by our study. We run the program keeping all other values of the parameters same as before for infected and Co- infected individuals.

The simulation's outcome under these conditions is depicted in Figure 6 (a) which indicates that the predicted total number of inpatients co-infected with COVID-19 and diabetes is more rapidly increased than only the COVID-19-infected population if the vaccination strategy is not executed. The expected total number of inpatients, only those with COVID-19, is more swiftly increased recovered than those co-infected with COVID-19 and diabetes population when the vaccination strategy is not applied, which is presented in Figure 6(b).

In epidemiology, disease spread and persistence are closely tied to the basic reproduction number and the endemic equilibrium point. This reproduction number is a marker for the initial dissemination of an ailment among a susceptible population, quantifying the average number of follow-on infections from a singular infected person introduced to a previously uninfected group. The spread of the coronavirus will diminish if R_0 is under 1, but will sustain if R_0 is above 1. To identify the key parameters affecting the coronavirus transmission, we ran a program using initial and parameter values detailed in Tab.1. The outcomes from this analysis are captured in Figures 6-9.

 doi:10.20944/preprints202406.1320.v1

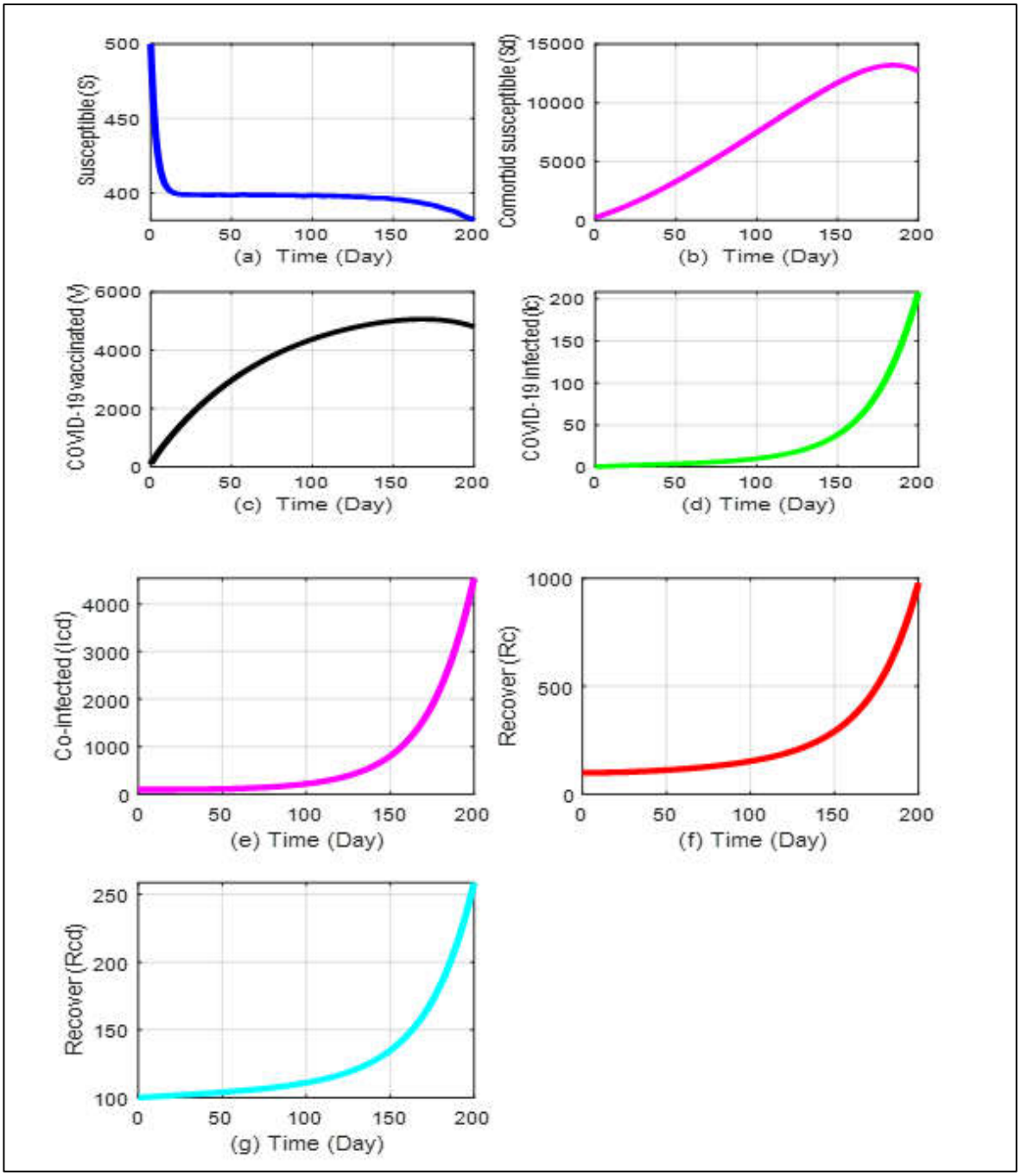

Figure 5. Simulations of the population over a period of 200 days when the basic reproduction rate is higher than 1. (a) Susceptible individuals, (b) Comorbid susceptible individuals, (c) COVID-19 vaccinated individuals, (d) COVID-19 infected individuals, (e) Co-infected individuals, (f) Recovered from COVID-19 only (g) Recovered from both COVID-19 and comorbid conditions .

Preprints.org (www.preprints.org) | NOT PEER-REVIEWED | Posted: 19 June 2024 doi:10.20944/preprints202406.1320.v1

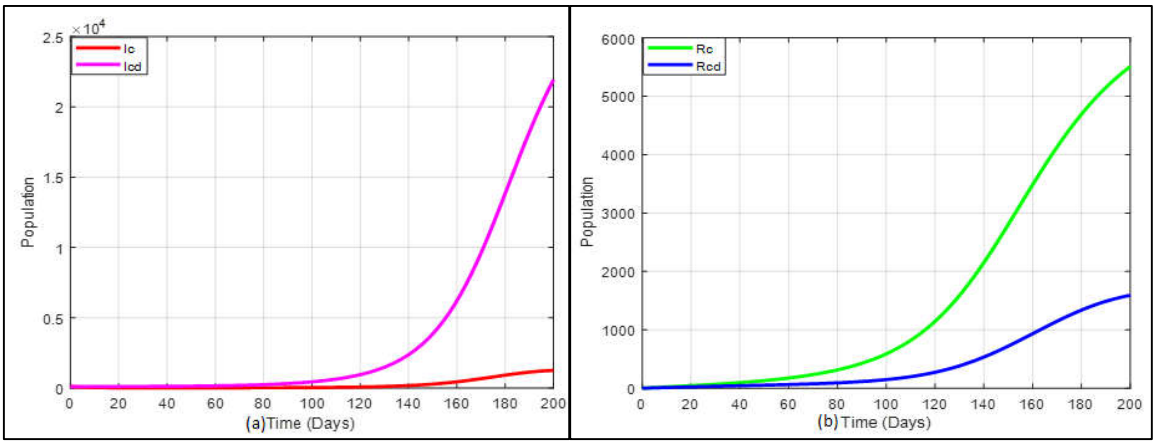

Figure 6. (a) Comparison of infected of COVID-19 only and co -infected COVID-19 with diabetics, (b) Comparison of recovered from COVID-19 only and co-infected COVID-19 with diabetics.

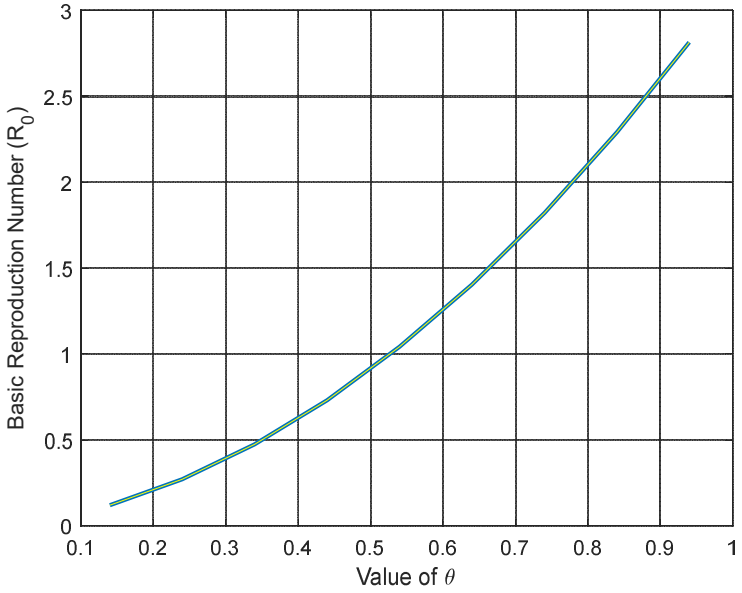

Figure 7. The value of R_0 is increased to the diabetes rate θ in vaccinated susceptible persons.

 doi:10.20944/preprints202406.1320.v1

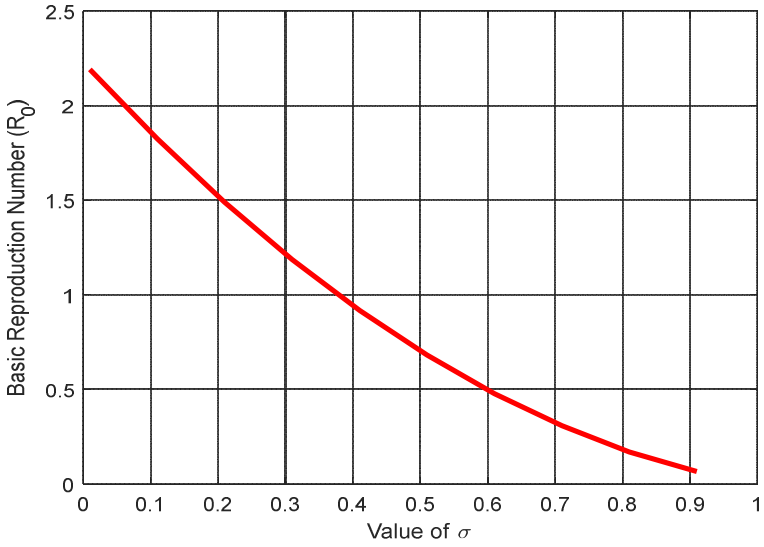

Figure 8. Demonstrates a decline in the value of R_0 corresponding to the efficacy rate σ of the COVID-19 vaccine.

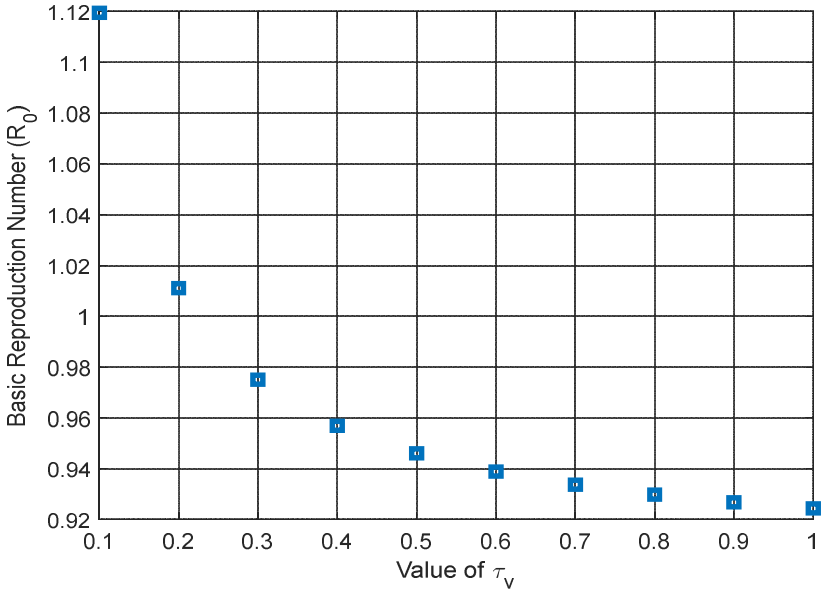

Figure 9. The decline in R_0 value in relation to the rise in COVID-19 vaccination rate τ_v.

 doi:10.20944/preprints202406.1320.v1

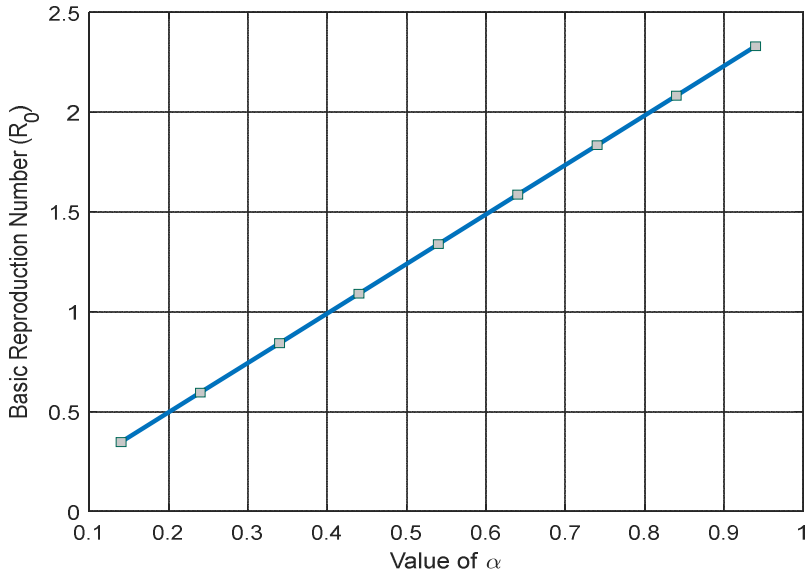

Figure 10. Visualization of the basic reproduction number in connection with the COVID-19 contact rate α.

Figures 7-10 illustrate how the basic reproduction number changes in relation to key parameters that influence the ongoing pandemic. Specifically, Figures 7 indicates that as the rate of diabetes (θ) rises in vaccinated susceptible individuals, the basic reproduction number surges exponentially, suggesting the disease's continued presence in the community. Figures 8 and 9 highlight a significant reduction in the basic reproduction number when considering the COVID-19 vaccine's efficacy rate (σ) and the growth in the vaccination rate (τ_v). Meanwhile, Figure 10 depicts a linear increase in the basic reproduction number as the COVID-19 contact rate (α) climbs.

The Influence of Vaccination

Figure 11 (a) shows the results related to the effects of vaccination. When τ_v is 0, it means there is no vaccination taking place. From the current data, it seems that our rate of vaccination isn't drastically reducing the number of COVID-19 cases. However, when we look closer at Figure 11 (a), as more people get vaccinated, the number of infections starts to drop slowly. It is interesting to note that for people with diabetes, COVID-19 cases still rise a bit even with a moderate vaccination rate ($\tau_v = 0.10$). But, when more people are vaccinated at a higher rate ($\tau_v = 0.20$), the number of infections reduces, which is also shown in Figure 11(b).

The vaccine's efficacy is also a vital factor in eliminating the disease. In Figure 12(a) shows a marked reduction in the number of COVID-19-infected cases as the vaccine efficacy increases. With higher vaccine efficacy (σ=0.70), the infection rate significantly decreases, demonstrating the vaccine's crucial role in controlling the pandemic. This suggests that effective vaccination campaigns can substantially mitigate the spread of COVID-19. On the other hand, the graph 12(b) illustrates that higher vaccine efficacy also reduces the number of co-infected cases of COVID-19 and diabetes. Over a long-term period, as vaccine efficacy increases, the incidence of co-infection decreases. This underscores the importance of high-efficacy vaccines in protecting diabetic patients, who are more vulnerable to severe outcomes.

Preprints.org (www.preprints.org) | NOT PEER-REVIEWED | Posted: 19 June 2024 doi:10.20944/preprints202406.1320.v1

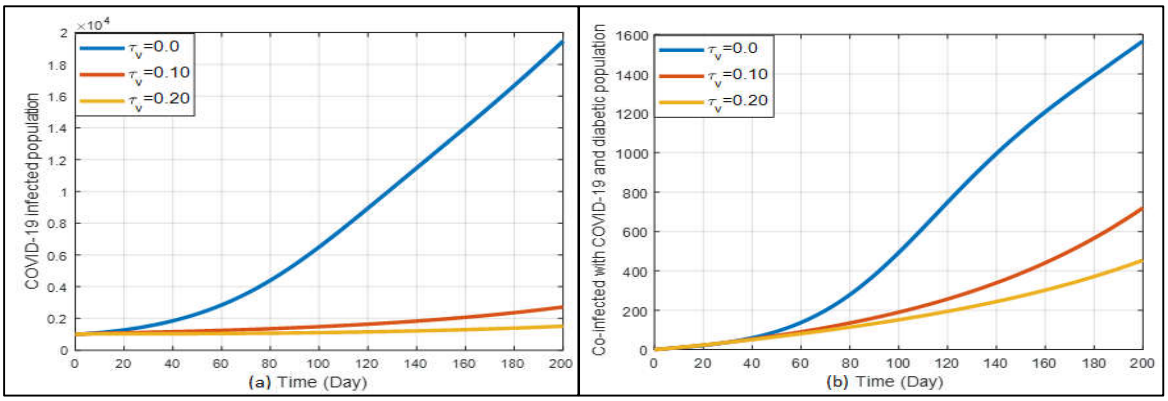

Figure 11. (a) Simulations of infected case and (b) Co-infected case for different vaccination rate τ_v.

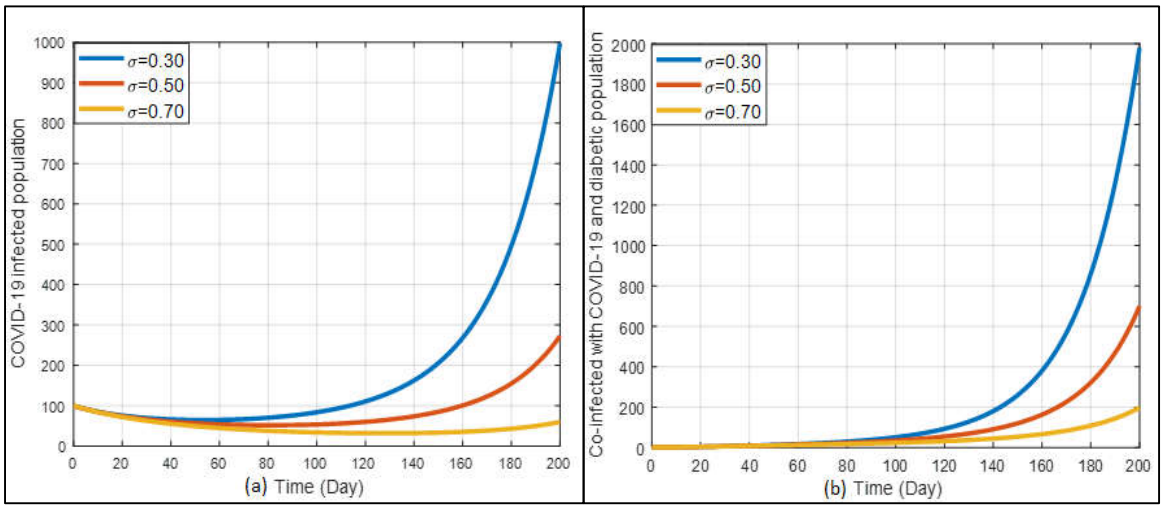

Figure 12. (a) Simulations of infected cases effect of COVID-19 and (b) Co-infected cases of COVID-19 for various vaccine efficacy σ.

Figure 13 displays the changing trajectories for three states: vaccination, COVID-19 infection, and co-infection with COVID-19 and diabetes. Notably, as the rate of vaccination rises, there's a marked decrease in the number of individuals infected with COVID-19 and those co-infected with both the virus and diabetes. But when the vaccination rate is decreasing, the infected population and co-infected with COVID-19 and diabetes are increasing.

In Figure 14(a), the relationship between the vaccination rate and the COVID-19-infected population is depicted. As the vaccination rate increases, there is a noticeable decline in the number of individuals infected with COVID-19. This highlights the effectiveness of increasing vaccination rates in controlling and reducing the spread of the virus. Similarly, Figure 14(b) shows an inverse relationship between the vaccination rate and the co-infected population with COVID-19 and diabetes. As vaccination rates rise, the number of co-infected individuals significantly decreases. These figures clearly demonstrate that higher vaccination rates effectively reduce the spread of COVID-19 and its co-infections. The marked reduction in both COVID-19 cases and co-infections with increased vaccination underscores the crucial role of vaccination in disease control.

Preprints.org (www.preprints.org) | NOT PEER-REVIEWED | Posted: 19 June 2024 doi:10.20944/preprints202406.1320.v1

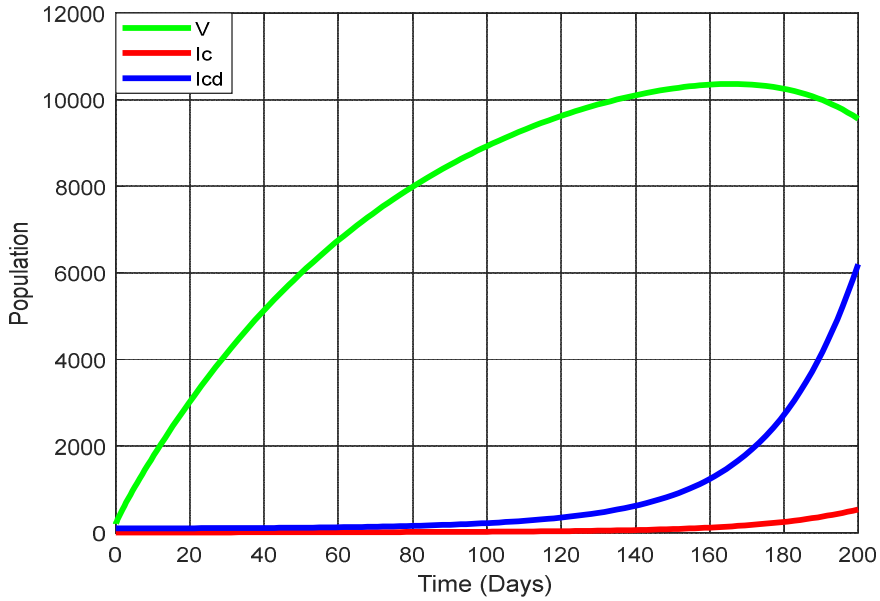

Figure 13. Simulations of incidence case effect of vaccination.

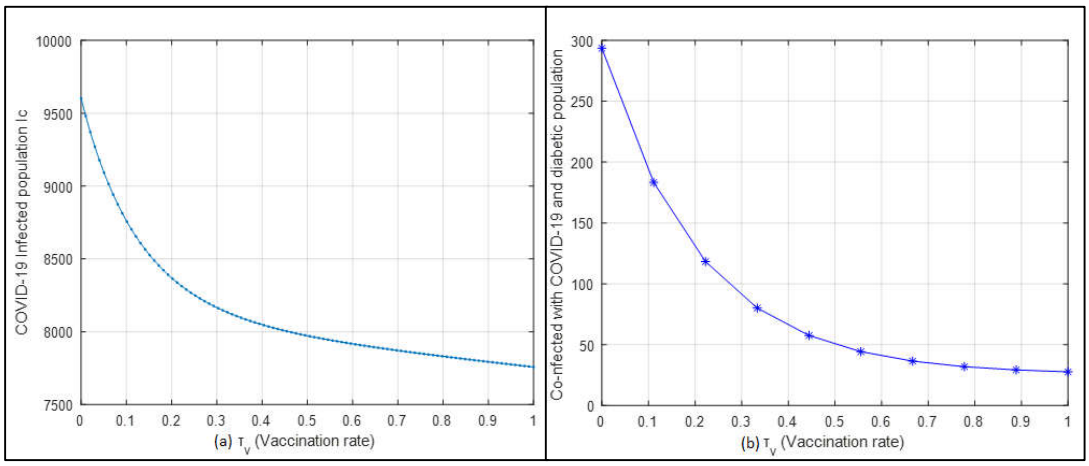

Figure 14. (a) Role of vaccination on COVID-19 infected population(I_C); (b) Role of vaccination on COVID-19 co-infected population (I_{Cd}).

5. Conclusions

We crafted a mathematical framework to assess the influence of vaccination on individuals co-infected with COVID-19 and diabetes. The study emphasized how the spread of COVID-19 has significant adverse effects on public health. We further investigated the impact of vaccination on the effectiveness of infection on the co-infection of COVID-19 and diabetes. Moreover, the critical vaccination threshold is derived, and it is underlined that even if a significant proportion of the population obtains vaccination. The following list includes the main conclusions of the new development model:

- An increased rate of transmission significantly impacts the disease's spread.
- A reproduction number less than one could lead to a disease-free equilibrium, making it globally unstable.
- The importance of the critical vaccination threshold was highlighted. Even high vaccination rates might not eliminate the disease if vaccine efficacy and disease reproduction are low.
- Vaccinations have been empirically reduce disease spread successfully.
- A significant inverse relationship was observed in our study between the vaccination rate and the incidence of both COVID-19 and its co-infections with diabetes.

 doi:10.20944/preprints202406.1320.v1

- While co-infections were evident, the severity or complexity of the co-infection between COVID-19 and diabetic complications remained consistent, without any observed intensification.

The findings reached through the sensitivity analysis are aligned with the observations made using the model, with a specific emphasis on how crucial transmission affects the progress of the disease. The findings support broad COVID-19 vaccination drives begun by the government, with a focus on diabetics. The current findings and models also maximise the advantages of simulation modelling to reduce COVID-19 and diabetes disease's global health complexity. Research directions in the future can concentrate on the effectiveness of different vaccination doses among various human races.

Acknowledgments: We would like to express our endless gratitude to Bangladesh University of Engineering and Technology (BUET) primary research fund for its continuous logistic and financial support and valuable insights during this research.

Author Contributions: Md. Abdul Hye and Md. Haider Ali Biswas: conceptualization, formal analysis, software, and original draft preparation. Md. Abdul Hye and Mohammed Forhad Uddin: methodology. Mohammed Forhad Uddin and Md. Haider Ali Biswas: validation and investigation and resources. Md. Abdul Hye: data curation. Mohammed Forhad Uddin: review and editing. Mohammed Forhad Uddin and Md. Haider Ali Biswas: supervision. All the authors have read and agreed to the published version of the manuscript.

Data Statement Availability: Data will be available upon request.

Conflicts of Interest: The authors declare that there are no conflicts of interest regarding the publication of this manuscript.

References

1. W.H. Organization, World Health Organization coronavirus disease (COVID-19) dashboard, World Health Organization, (2020).
2. P. Zhou, X.-L. Yang, X.-G. Wang, B. Hu, L. Zhang, W. Zhang, H.-R. Si, Y. Zhu, B. Li, C.-L. Huang, Addendum: A pneumonia outbreak associated with a new coronavirus of probable bat origin, Nature, 588 (2020) E6-E6.
3. M. Nicola, Z. Alsafi, C. Sohrabi, A. Kerwan, A. Al-Jabir, C. Iosifidis, M. Agha, R. Agha, The socio-economic implications of the coronavirus pandemic (COVID-19): A review, International journal of surgery, 78 (2020) 185-193.
4. A. Egonmwan, D. Okuonghae, Mathematical analysis of a tuberculosis model with imperfect vaccine, International Journal of Biomathematics, 12 (2019) 1950073.
5. F.P. Polack, S.J. Thomas, N. Kitchin, J. Absalon, A. Gurtman, S. Lockhart, J.L. Perez, G. Pérez Marc, E.D. Moreira, C. Zerbini, Safety and efficacy of the BNT162b2 mRNA Covid-19 vaccine, New England journal of medicine, 383 (2020) 2603-2615.
6. P. Van den Driessche, J. Watmough, Reproduction numbers and sub-threshold endemic equilibria for compartmental models of disease transmission, Mathematical biosciences, 180 (2002) 29-48.
7. C.M. Gomes, L.A. Favorito, J.V.T. Henriques, A.F. Canalini, K.M. Anzolch, R.d.C. Fernandes, C.H. Bellucci, C.S. Silva, M.L. Wroclawski, A.C.L. Pompeo, Impact of COVID-19 on clinical practice, income, health and lifestyle behavior of Brazilian urologists, International braz j urol, 46 (2020) 1042-1071.
8. A. Azeez, J. Ndege, R. Mutambayi, Y. Qin, A mathematical model for TB/HIV co-infection treatment and transmission mechanism, Asian J. Math. Computer Res, 22 (2017) 180-192.
9. H. Tasman, An optimal treatment control of TB-HIV coinfection, International Journal of Mathematics and Mathematical Sciences, 2016 (2016).
10. K. Bjorgul, W.M. Novicoff, K.J. Saleh, Evaluating comorbidities in total hip and knee arthroplasty: available instruments, Journal of orthopaedics and traumatology, 11 (2010) 203-209.
11. E. Gurmu, B. Bole, P. Koya, A Mathematical model for co-infection of HPV and HSV-II with drug resistance compartment, Int. J. Sci. Res. in Mathematical and Statistical Sciences Vol, 7 (2020).
12. D. Cucinotta, M. Vanelli, WHO declares COVID-19 a pandemic, Acta bio medica: Atenei parmensis, 91 (2020) 157.
13. M.H.A. Biswas, L.T. Paiva, M.D.R. de Pinho, A SEIR model for control of infectious diseases with constraints, Mathematical Biosciences and Engineering, 11 (2014) 761-784.
14. H. Ali Biswas, On the evolution of AIDS/HIV treatment: an optimal control approach, Current HIV Research, 12 (2014) 1-12.
15. L.-M. Cai, Z. Li, X. Song, Global analysis of an epidemic model with vaccination, Journal of Applied Mathematics and Computing, 57 (2018) 605-628.

 doi:10.20944/preprints202406.1320.v1

16. A. Omame, U.K. Nwajeri, M. Abbas, C.P. Onyenegecha, A fractional order control model for Diabetes and COVID-19 co-dynamics with Mittag-Leffler function, Alexandria Engineering Journal, 61 (2022) 7619-7635.
17. Y. Bai, L. Yao, T. Wei, F. Tian, D.-Y. Jin, L. Chen, M. Wang, Presumed asymptomatic carrier transmission of COVID-19, Jama, 323 (2020) 1406-1407.
18. O.J. Watson, G. Barnsley, J. Toor, A.B. Hogan, P. Winskill, A.C. Ghani, Global impact of the first year of COVID-19 vaccination: a mathematical modelling study, The Lancet Infectious Diseases, 22 (2022) 1293-1302.
19. H.-A.H. Dang, M.N. Do, COVID-19 Pandemic and the Health and Well-being of Vulnerable People in Vietnam, in, GLO Discussion Paper, 2022.
20. R. Prieto Curiel, H. González Ramírez, Vaccination strategies against COVID-19 and the diffusion of anti-vaccination views, Scientific Reports, 11 (2021) 6626.
21. E.A. Iboi, C.N. Ngonghala, A.B. Gumel, Will an imperfect vaccine curtail the COVID-19 pandemic in the US?, Infectious Disease Modelling, 5 (2020) 510-524.
22. B. Tang, X. Wang, Q. Li, N.L. Bragazzi, S. Tang, Y. Xiao, J. Wu, Estimation of the transmission risk of the 2019-nCoV and its implication for public health interventions, Journal of clinical medicine, 9 (2020) 462.
23. H. Zhu, L. Wei, P. Niu, The novel coronavirus outbreak in Wuhan, China, Global health research and policy, 5 (2020) 1-3.
24. S.A. Pedro, F.T. Ndjomatchoua, P. Jentsch, J.M. Tchuenche, M. Anand, C.T. Bauch, Conditions for a second wave of COVID-19 due to interactions between disease dynamics and social processes, Frontiers in Physics, 8 (2020) 574514.
25. T.K. Irena, S. Gakkhar, A dynamical model for HIV-typhoid co-infection with typhoid vaccine, Journal of Applied Mathematics and Computing, (2021) 1-30.
26. H. Askari, N. Sanadgol, A. Azarnezhad, A. Tajbakhsh, H. Rafiei, A.R. Safarpour, S.M. Gheibihayat, E. Raeis-Abdollahi, A. Savardashtaki, A. Ghanbariasad, Kidney diseases and COVID-19 infection: causes and effect, supportive therapeutics and nutritional perspectives, Heliyon, 7 (2021).
27. M. Dadashi, S. Khaleghnejad, P. Abedi Elkhichi, M. Goudarzi, H. Goudarzi, A. Taghavi, M. Vaezjalali, B. Hajikhani, COVID-19 and influenza co-infection: a systematic review and meta-analysis, Frontiers in medicine, 8 (2021) 681469.
28. G.T. Mousquer, A. Peres, M. Fiegenbaum, Pathology of TB/COVID-19 co-infection: the phantom menace, Tuberculosis, 126 (2021) 102020.
29. Lakshmikantham, S., Leela, S., and Martynyuk, A. A., Stability Analysis of Nonlinear Systems, Marcel Dekker, Inc., New York, 1989.
30. McCall J, Genetic algorithms for modelling and optimisation, J. Comput. Appl. Math. 184 (2005) 222
31. Okuonghae D, Omame A, Analysis of a mathematical model for COVID-19 population dynamics in Lagos, Nigeria, Chaos Solitons Fractals 139(2020) 110032.
32. Omame, A., Sene, N., Nometa, I., Nwakanma, C. I., Nwafor, E. U., Iheonu, N. O., & Okuonghae, D. (2021). Analysis of COVID-19 and comorbidity co-infection model with optimal control. Optimal Control Applications and Methods, *42*(6), 1568-1590.